25th ABCM International Congress of Mechanical Engineering
October 20-25, 2019, Uberlândia, MG, Brazil

COB-2019-1568
COHERENT STRUCTURES IN NON-NEWTONIAN POWER LAW FLUIDS IN RECTANGULAR CHANNELS

Cristian Mauricio Potosi Rosero
Leonardo José Castellanos
Juliana Braga Rodrigues Loureiro
Interdisciplinary Center for Fluid Dynamics, Federal University of Rio de Janeiro. Av. Moniz de Aragão 360, 21941-594 Rio de Janeiro, Brazil.
cristian.potosi@nidf.ufrj.br
leonardo.castellanos@nidf.ufrj.br
jbrloureiro@mecanica.coppe.ufrj.br

David Dennis
Depart. of Mechanical, Materials & Aerospace Engineering. University of Liverpool, Liverpool L69 3BX, United Kingdom.
david.dennis@liverpool.ac.uk

Abstract. *This work applies a method to identify very large scale motions in Newtonian and Non-Newtonian turbulent flows. A 0.1% weight concentration of Carboxymethyl Cellullose (CMC) were used to simulate the behavior of a Non-Newtonian Power Law fluid ($n = 0.5457$). The characteristics of the flow were measured through a Stereoscopic Particle Image Velocimetry in a rectangular channel section. Information about streamwise velocity and turbulent kinetic energy profiles are presented subsequently. In particular, the reconstruction of large scale motions, also known as coherent structures, is performed. These results are of substantial importance to the understanding of the turbulence problem and the changes in the boundary layer morphology.*

Keywords: *Coherent structures, Non-Newtonian Fluids, Boundary layer.*

1. INTRODUCTION

The structure of the boundary layer in Non-Newtonian fluids was of particular interest for researchers in the latest years. The asymptotic structure of the attached boundary layer was originally advanced by Prandtl (1925) and Von Karman (1930). They propose that the flow structure can be divided into two layers: a wall viscous layer, in which the turbulent and laminar stresses are of comparable magnitude and a defect layer, in which the velocity profile may be expressed in terms of a small perturbation to the external flow solution. The work of Loureiro and Silva Freire (2013) showed that for power law fluids, the thickness of the viscous sublayer depends on the index of power-law models, n.

Some authors made evident the existence of long structures in the streamwise direction of the flow. That is the case of Dennis and Nickels (2009), that developed and applied a method to identify very large scale motions. This method uses the Taylor's frozen turbulence hypothesis (Taylor, 1938) to obtain long meandering structures in the log-region of a turbulent boundary layer, using spatial information from Stereoscopic Particle Image Velocimetry measurements. These authors showed that the method was valid for moderate projection distances.

A strong relation between the very large scale motions and the turbulent parameters found in the fluid motivates the analysis of coherent structures with the propose of explain phenomenons that depends on the boundary layer morphology. As shown by Balakumar and Adrian (2007), a big portion of the turbulent kinetic energy (40 to 60%) and the Reynolds stresses (30 to 50%) are contained in these structures.

Several works based on the identification of turbulent structures were developed recently, most of them analyzing the distribution existing in Newtonian laminar and turbulent flows in pipes. A very close distribution is observed in the case of channels (Lee *et al.*, 2015), just modifying the structure length being longer for these last.

The main objective of this work is to analyze the distribution and main characteristics of the coherent structures close to the wall and their effect in the behavior of the boundary layer structure for purely viscous Non-Newtonian fluids.

2. EXPERIMENTAL PROCEDURE

The experimental setup is composed by a 3.3 m long plexiglass rectangular channel (Fig. 1). The test cross sectional area is 150x20 mm^2 and it is located at $x/h = 50$ downstream from the inlet to ensure a fully developed flow. The flow rate used in the experiments was 9.6 m^{3}h^{-1}. For this flow rate a concentration 0.1% of Carboxymethyl Sodium Cellulose (CMC) in water were used to simulate the behavior of the power law fluid to be compared with the water flow. The index n of this power-law flow was equal to 0.5457.

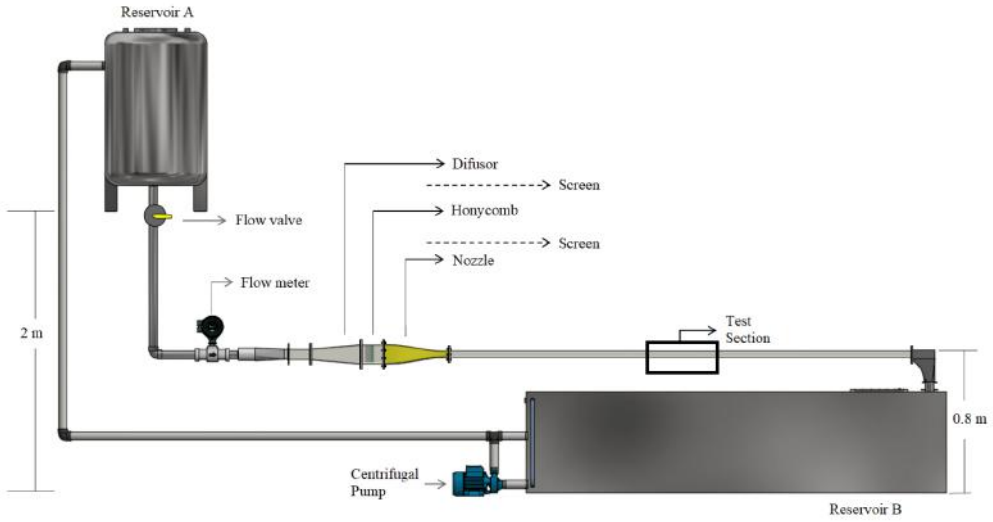

Figure 1. Experimental setup.

The water channel is equipped with a honeycomb, a diffuser, three fine grids and a settling chamber in order to straighten the flow and remove any mean swirl. A 6.5:1 contraction is used upstream of the test section to further reduce the turbulence intensity by accelerating the mean flow.

The channel operates in a closed loop, in which the fluid is fed from a reservoir located 3 m above. The liquid level in the reservoir is kept constant by a system of valves and a 2 HP centrifugal pump. The flow rate, measured by an EH Magnetic Flowmeter, is kept constant and with a maximum variation of 1% of the mean flow. A filter is placed just after the pump to avoid possible impurities and contamination that could affect the optical measures.

The Stereoscopic Particle Image Velocimetry system (Fig.2) was composed by a high frequency diode pumped Nd:YLF, dual cavity laser, with output energies of up to 15 mJ, a wavelength of 527 nm and a maximum frequency of 10 kHz. The flow is seeded with Silver coated hollow glass spheres with a mean particle diameter of 20 μm.

Figure 2. Stereoscopic Particle Image Velocimetry Setup.

The light reflected by the particles was recorded by two CCD cameras. These cameras have a 1920 x 1200 pixels, 12 bit resolution and a minimum inter-frame time of 1.4 μs. The acquisition frequency was set to 600 Hz. In this

configuration two lenses Nikon AF Micro Nikkor 105 mm $f/2.8D$ were used. Two triangular boxes, filled with the same working fluid, were located in the lateral walls of the channel to reduce optical distortions. The cameras were located at a $\pm$ 45 degree angle in relation to the channel center line. This setup allows the reconstruction of a 3D portion of the flow at a cross section of the channel. A multilevel target was used to do the calibration of the images to get an accurate reconstruction of the velocity vectors. This calibration process is fundamental to reduce measurement errors. Misalignments greater than 2% of the total characteristic length will lead to large errors as shown in Nezu and Sanjou (2011). Image post-processing was performed by the Dynamic Studio software.

3. RESULTS

The results for the Stereoscopic Particle Image Velocimetry are shown in Fig. 3 and 4. The fields for the streamwise mean velocity U and the turbulent kinetic energy k for both fluids are presented. Fig. 5 shows U and k profiles in the center of the channel. The difference in the peak velocity between water and the non-Newtonian fluid is the result of the pressure drop due this fluid. For water, the maximum velocity is closed to 1.0, in the other hand, for CMC, the velocity is 1.1. The velocity values were dimensionless dividing by the bulk velocity U_b, and for k, the square of this velocity was used.

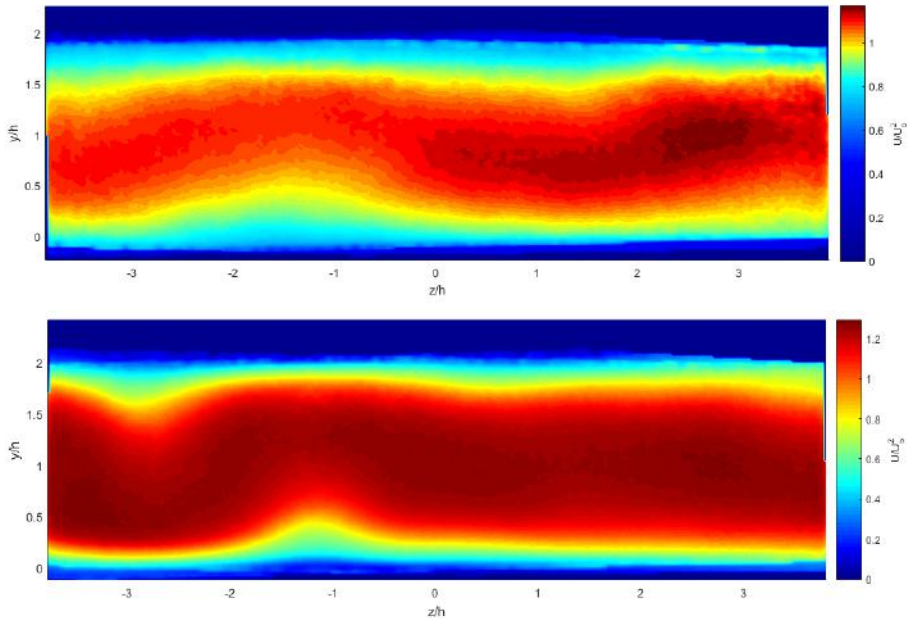

Figure 3. Streamwise mean velocity fields for water (top) and Power law fluid $n = 0.5457$ (bottom). Flow rate condition: 9.6 m^3 h^{-1}.

To a better understanding of the near-wall motion, some turbulent statistics must be studied meticulously. The coherent structures embed information about the Reynolds stresses, so that the analysis of their properties may explain the changes of the boundary layer observed for Non-Newtonian fluids.

The streamwise velocity fluctuations at a plane parallel to the wall are presented in Fig.6. A slice for $y/h = 0.2$, where y denotes the distance from the wall, shows clear differences between the Newtonian flow (top) and the 0.1% CMC concentration (bottom). The red structures represent positive fluctuations and the blue ones are related to negative fluctuations.

In the case of the water flow, a constant pattern is not observed on the distribution of the structures. There are short packages (not more than 20h length) of positive fluctuations very close to each other, which are interrupted by the presence of the negative motions. For the Non-Newtonian case, the changes in the fluid rheology induce changes in the viscous sublayer. These changes are highly influential on the organization of the flow in the fully turbulent region. The structures along the channel are very well organized, continuous and with a length longer than 100h.

Figure 7 shows two-point spatial correlation plots for Newtonian fluid (top) and Non-Newtonian fluid (bottom). The red contours denote a positive level of correlation and the blue ones represent a negative correlation. This result shows that the power law fluid rheology produces structures so much better correlated compared with water. The turbulent effects close to the wall are attenuated and new organized packages appear in this region.

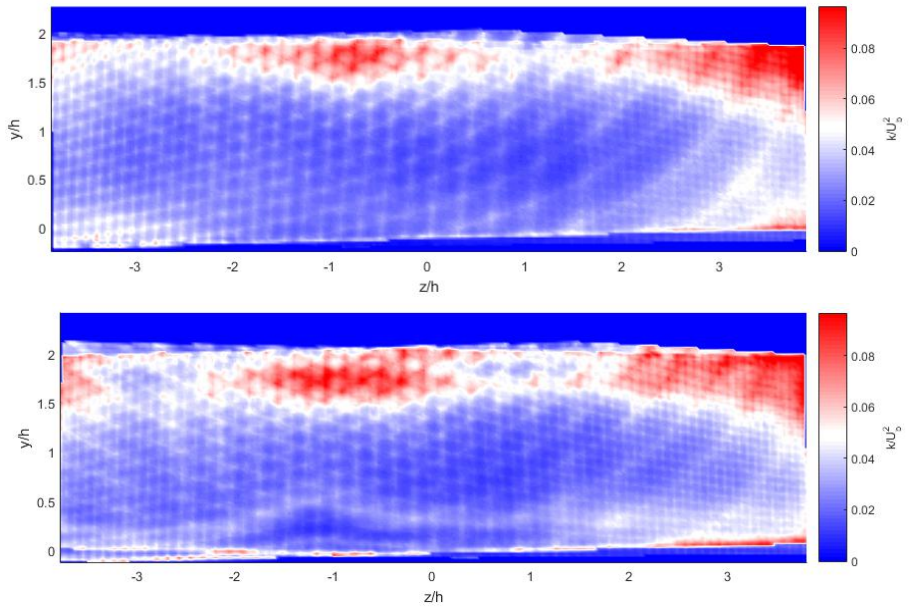

Figure 4. Turbulent kinetic energy fields for water (top) and Power law fluid $n = 0.5457$ (bottom). Flow rate condition: 9.6 m^3 h^{-1}.

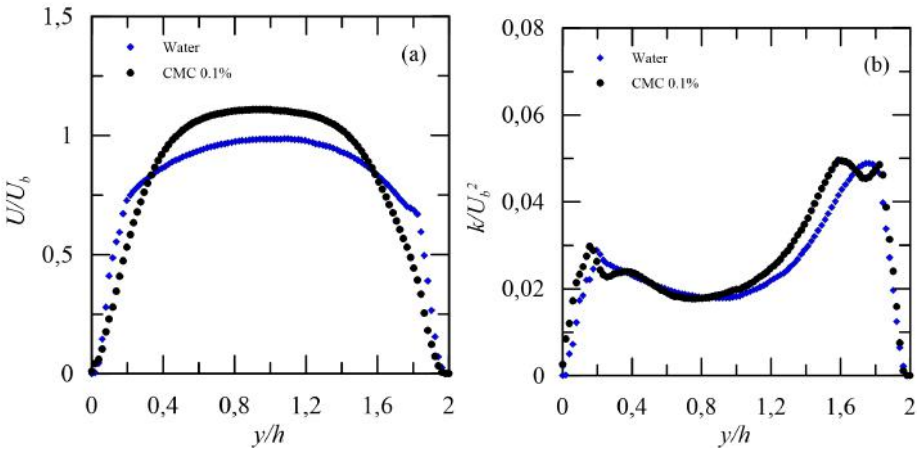

Figure 5. (a) Streamwise mean velocity profiles in the center of the channel. (b) Turbulent kinetic energy profiles in the center of the channel.

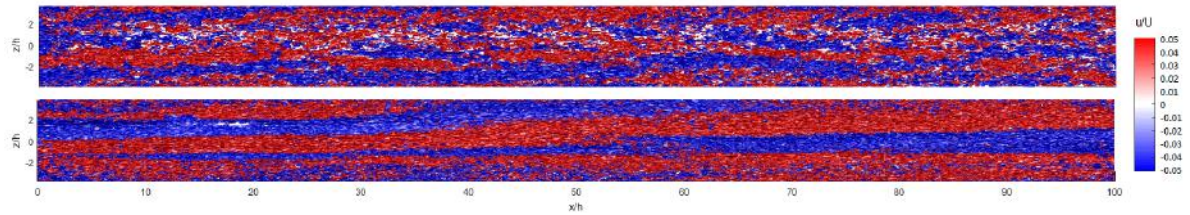

Figure 6. Wall parallel slice of the 3D coherent structure reconstruction in $y/h = 0.2$ for water (top) and a 0.1% CMC concentration (bottom). Flow rate condition: 9.6 m^3 h^{-1}.

4. CONCLUSIONS

Taylor's frozen turbulence hypotheses can be used to reconstruct pseudo-instantaneous fields of streamwise velocity fluctuations from StereoPIV measurements. For power law fluids, changes in the viscous region are highly influential on the organization of the flow in the fully turbulent region, with the establishment of very stable and long turbulent structures. The turbulent structures are a strong tool to improve the understanding of phenomenons that depend on modifications in the viscous sub-layer affecting the logarithmic region directly.

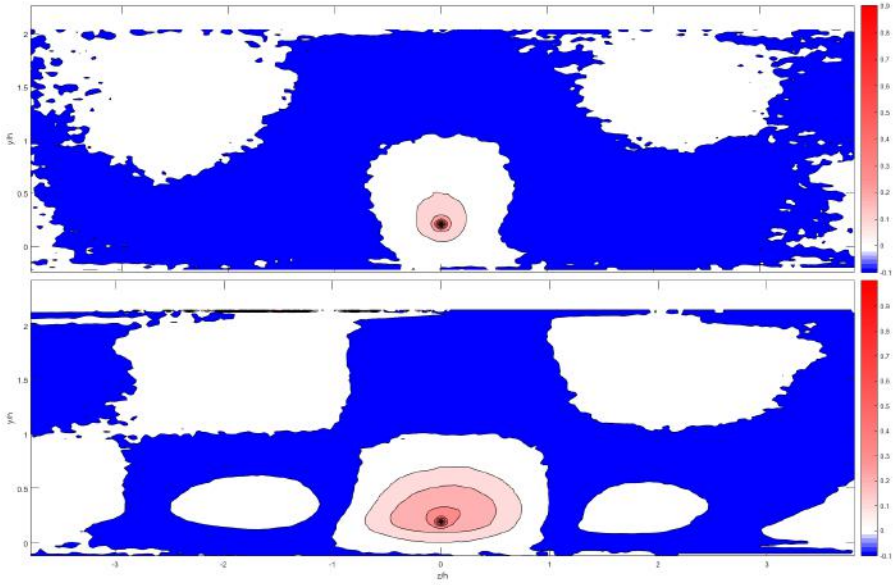

Figure 7. Spacial correlation in cross-stream plane in $y/h = 0.2$ for water (top) and a 0.1% CMC concentration (bottom). Flow rate condition: 9.6 m^3 h^{-1}.

5. ACKNOWLEDGEMENTS

CMPR and LJC are thankful for Petrobras/ANP for their MSc scholarship and research sponsorship. JBRL benefited from a CNPq Research Fellowship (Grant No 309455/2016-2) and from further financial support through Grants CNPq 458249/2014-9 and FAPERJ E-26/203.257/2016.

6. REFERENCES

Balakumar, B.J. and Adrian, R.J., 2007. "Large and very-large-scale motions in channel and boundary-layer flows". *Phil. Trans. R. Soc. Lond.*, Vol. 365, pp. 665–681.

Dennis, D.J.C. and Nickels, T.B., 2009. "3d structures from stereoscopic piv measurements in a turbulent boundary layer". *Peinke J., Oberlack M., Talamelli A. (eds) Progress in Turbulence III. Springer Proceedings in Physics*, Vol. 131, pp. 65–68.

Lee, J., Ahn, J. and Sung, H.J., 2015. "Comparision of large- and very-large-scale motions in turbulent pipe and channel flows". *Phys. Fluids*, Vol. 27, p. 025101.

Loureiro, J.B.R. and Silva Freire, A.P., 2013. "Asymptotic analysis of turbulent boundary layer flow of purely viscous non-newtonian fluids". *Journal of Non-Newtonian Fluid Mechanics*, Vol. 199, pp. 20–28.

Nezu, I. and Sanjou, M., 2011. "Piv and ptv measurements in hydro-sciences with focus on turbulent open-channel flows". *J Hydro-Environ. Res*, Vol. 5, pp. 215–230.

Prandtl, L., 1925. "Bericht uber untersuchungen zur ausgebildeten turbulenz". *Z. Angew. Math. Mech.*, Vol. 5, pp. 136–139.

Taylor, G.I., 1938. "The spectrum of turbulence". *Proceeding of the Royal Society of London. Series A, Mathematical and Physical Sciences*, Vol. 164, pp. 476–490.

Von Karman, T., 1930. "Mechanische ahnlichkeit und turbulenz". *Nachrichten Von der Gesellschaft der Wissenschaften zu Gottingen, Mathematisch- Physikalische Klasse*, pp. 476–490.

7. RESPONSIBILITY NOTICE

The authors are the only responsible for the printed material included in this paper.